RESEARCH ARTICLE
doi:10.59236/geomorphica.v2i2.56

GEOMORPHICA

Nested, Reach-Scale Fluvial Sediment Budgets Quantify Watershed Sediment Transport Pathways

James E. Pizzuto *[1], **Kristen Cribb**[2], **Anne Kelly**[3]

[1]Department of Earth Sciences, University of Delaware, Newark, DE, USA, [2]Biomedical Engineering Department, University of Delaware, Newark, DE, USA, [3]AES Corporation, Arlington, VA, USA

Author contributions: *Conceptualization*: J.E.P.. *Data curation*: J.E.P., K.C., A.K.. *Formal analysis*: J.E.P., K.C., A.K.. *Funding acquisition*: J.E.P.. *Investigation*: J.E.P., K.C.. *Methodology*: J.E.P.. *Project administration*: J.E.P.. *Resources*: J.E.P.. *Software*: J.E.P.. *Supervision*: J.E.P.. *Validation*: J.E.P.. *Visualization*: J.E.P.. *Writing – original draft*: J.E.P.. *Writing – review & editing*: J.E.P., K.C., A.K..

Abstract Watershed sediment budgets sum sediment sources (bank erosion and tributaries) and subtract sediment sinks (floodplains) to compute the watershed sediment output. Because computations are lumped, however, these budgets cannot quantify contributions from individual sources to the watershed output. We overcome this limitation by dividing the channel network into nested reaches, each with its own sediment budget. The nested framework partitions sediment between transport and storage as it moves downstream, quantifying the contributions from individual sources to watershed outputs. We quantify sediment fluxes using gaging station data, sediment fingerprinting, hydrodynamic modeling, geomorphic mapping, and measured rates of erosion and deposition. Bank erosion supplies 15 790 Mg/yr to the watershed budget, while upland hillslopes contribute 6 300 Mg/yr, with 10 380 Mg/yr stored on floodplains. The output computed from the budget (11 710 Mg/yr) is within the uncertainty of 9 300–43 000 Mg/yr of the measured output, so the budget balances. Reach-scale budgets identify local sediment hotspots, while routing computations indicate that bank erosion supplies 76 $\pm$ 5% of the watershed sediment flux, with upland hillslopes contributing 24 $\pm$ 3%. Legacy sediments comprise 34 $\pm$ 6% of the output. By quantifying individual source contributions to watershed sediment fluxes, the nested approach can improve sediment management decision-making.

Non-technical summary Excess sediment is a common water quality problem often addressed by mitigating watershed erosion hotspots. To identify erosion hotspots, geomorphologists produce sediment budgets, an accounting procedure that quantifies erosion, deposition, and transport variables, and relates them through mass balance. Sediment budgets sum erosional sources and subtract deposition to predict the sediment leaving a watershed. This approach, however, fails to connect specific sources to the outlet, because the individual sources that supply deposited sediment are unknown. We solve this problem by nesting 140 sediment budgets along the stream network of the White Clay Creek, southeastern Pennsylvania, USA. Each budget consists of sediment eroded from hillslopes and streambanks, sediment deposited on floodplains, and input and output channel sediment fluxes. By solving the mass balance of all the nested budget reaches simultaneously, the contribution of any individual sediment source to the watershed output can be quantified. Results indicate that bank erosion contributes 76% of the watershed sediment yield, with the remaining 24% from hillslope erosion. Eroded legacy sediments (deposits related to post-Colonial watershed disturbance) comprise 34% of the watershed sediment flux. The nested sediment budget approach provides a new, parsimonious method to quantify watershed-scale sediment transport patterns.

Received: July 16, 2025
Accepted: March 10, 2026
Published: June 9, 2026

1 Introduction

Understanding sediment sources, sinks, fluxes, and transport pathways is key to effective sediment management at the watershed scale (Frings and Ten Brinke, 2018). This information is needed to effectively locate Best Management Practices to reduce sediment loading (Noe et al., 2020), to understand the timing of sediment delivery (Reid and Dunne, 2016), and to evaluate lag times between management actions and the delivery of benefits in the form of reduced sediment loading to the watershed outlet (Meals et al., 2010; Pizzuto and Huffman, 2025).

Sediment budgets are the primary tool for geomorphologists to document watershed sediment processes (Reid and Dunne, 2016). Sediment budget analyses determine the relative magnitudes of potential sediment sources (erosion of channels, hillslopes, gullies, riverbanks, high bluffs, landslides, etc.) and potential sediment sinks (alluvial fans, toeslopes, floodplains, reservoirs, etc.). Summing inputs and subtracting outputs provides an estimate of the sediment flux leaving the watershed. Sediment budget studies have led to key scientific insights, including the role of floodplain and hillslope storage in moderating sediment yield following anthropogenic watershed disturbance (Costa, 1975; Knox, 2006; Trimble, 1981), how climate change influences long-term sediment yield (Church and Slaymaker, 1989), the importance of the sediment balance

*Corresponding author: pizzuto@udel.edu

in governing fluvial equilibrium (Grams and Schmidt, 2005), the impact of mining on fluvial systems (James et al., 2019), and other important results.

Mathematically, a sediment budget is a statement of conservation of mass applied to a specific region in space (i.e., a control volume) over a clearly defined time interval. Here we consider a control volume consisting of the entire channel network within a watershed, and assume that channels are connected to floodplains and other adjacent sediment storage reservoirs that serve as both sediment sinks (through deposition) and sediment sources (through erosion). Assuming that the channel network does not store sediment over relevant timescales, the sediment budget for the watershed consists of tributary inputs to the channel network, sediment losses and gains through exchanges with storage reservoirs, and sediment leaving the watershed.

$$\begin{aligned} Output\ sediment\ flux = {} & input\ flux_1 + input\ flux_2 \\ & + \cdots - deposition\ flux_1 \\ & - deposition\ flux_2 - \cdots \end{aligned} \tag{1}$$

While quantifying the terms of Eq. 1 provides clear estimates of the magnitudes of potential sediment transfers, the integrated nature of Eq. 1 has an important limitation: it fails to connect specific sediment sources to the output flux. This occurs because the supply from individual sources can be preferentially sequestered in sediment sinks through deposition, and preferentially replaced by sediment eroded from storage reservoirs. Thus, Eq. 1 does not determine the relative contribution of individual sources to the watershed output flux, so it may not identify where to focus remediation projects designed to reduce watershed sediment loading.

At least three strategies have been developed to connect sediment contributions from specific watershed locations to the watershed sediment output. One involves combining sediment budget analyses with sediment fingerprinting, allowing geochemical analyses of sediment delivered from the watershed to identify sediment from specific sources upstream (Belmont et al., 2014; Gellis and Walling, 2011; Rose et al., 2018a,b). However, sediment fingerprinting methods often require assumptions regarding sediment transport pathways that may not always be met (Karwan et al., 2018). Another approach is to use watershed sediment transport models to route sediment from specific source locations to the outlet of the basin (Bainbridge et al., 2023; Shenk and Linker, 2013). Watershed models can provide useful insights and predictions, but they require extensive calibration and most models commonly used in watershed applications neglect floodplain exchange and other important sediment processes (Borah et al., 2008). The third approach is to divide the watershed into subreaches and create nested sediment budgets, with the output from upstream reaches providing the input to neighboring downstream reaches (Turley et al., 2021, 2024). Nested sediment budgets can provide spatially explicit sediment flux estimates that in some cases allow sediment from specific source locations to be routed to the farthest outlet downstream. Sediment budgets have the compelling advantage of being grounded in measurements, rather than relying on poorly constrained sediment transport models or untested assumptions regarding sediment transport pathways.

This study presents a sediment budget for a 5th-order watershed in the mid-Atlantic U.S., a region where plans for restoring the Chesapeake Bay specifically focus on reducing the loading to the Bay from specific watershed sources (Langland and Cronin, 2003), a strategy that requires understanding how watershed locations may (or may not) be connected to the Chesapeake Bay downstream. Rather than developing a single integrated sediment budget for the entire watershed, we formulate individual budgets for 140 nested river reaches spanning the entire valley network from headwaters to the basin outlet. We show how this approach allows us to quantify the contributions of each individual sediment source to the cumulative sediment flux leaving the watershed. Our analysis demonstrates that approximately three-quarters of the sediment delivered from the watershed is supplied by bank erosion, a result that could not have been obtained from a traditional, spatially averaged sediment budget.

2 Study area

Data were collected in the White Clay Creek (WCC) watershed upstream of the U.S. Geological Survey's (USGS) gaging station White Clay Creek near Strickersville (USGS #01478245) in southeastern Pennsylvania, U.S.A. (Fig. 1). WCC has a drainage basin area of 153.3 km^2 at the Strickersville gaging station. Another USGS gaging station, East Branch White Clay Tributary near London Grove, PA (USGS #01478100), with a drainage basin area of 7.2 km^2, defines hydrologic inputs from White Clay Creek's headwaters.

The watershed of WCC has a moist, subtropical climate (Köppen-Geiger classification Cfa, Kottek et al., 2006) with moderately cold winters and warm, humid summers, averaging 1070 mm of annual precipitation (Corrozi et al., 2008). It is underlain by Paleozoic gneiss and schist of the Wissahickon Formation and the Cockeysville Marble (Pennsylvania Department of Conservation and Natural Resources, 2025; Ramsey, 2005). The study area is located within the Piedmont Physiographic Province (Fischer et al., 2004; Renner, 1927), and exhibits low-moderate relief (Hack, 1982). Agriculture (47%) and forest/wetlands (28%) are the primary land uses, with scattered suburban development (25%) (University of Delaware Water Resources Center, 2024); impervious cover in 2005 varied from 10–13% (Corrozi et al., 2008). A portion of WCC in the study area was designated a National Wild and Scenic River in 2000 (Interagency Wild and Scenic Rivers Council, 2025).

Rivers in the WCC watershed are semi-alluvial river channels, often confined laterally by valley walls and other non-alluvial landforms and vertically by bedrock exposures (Turowski et al., 2008; Bodek et al., 2021). Channels are mostly single-thread and sinuous but non-meandering, though side channels are common (Bodek et al., 2021). Bankfull widths range from 10–30 m, with bed slopes varying from 0.002–0.007 (McCarthy, 2018).

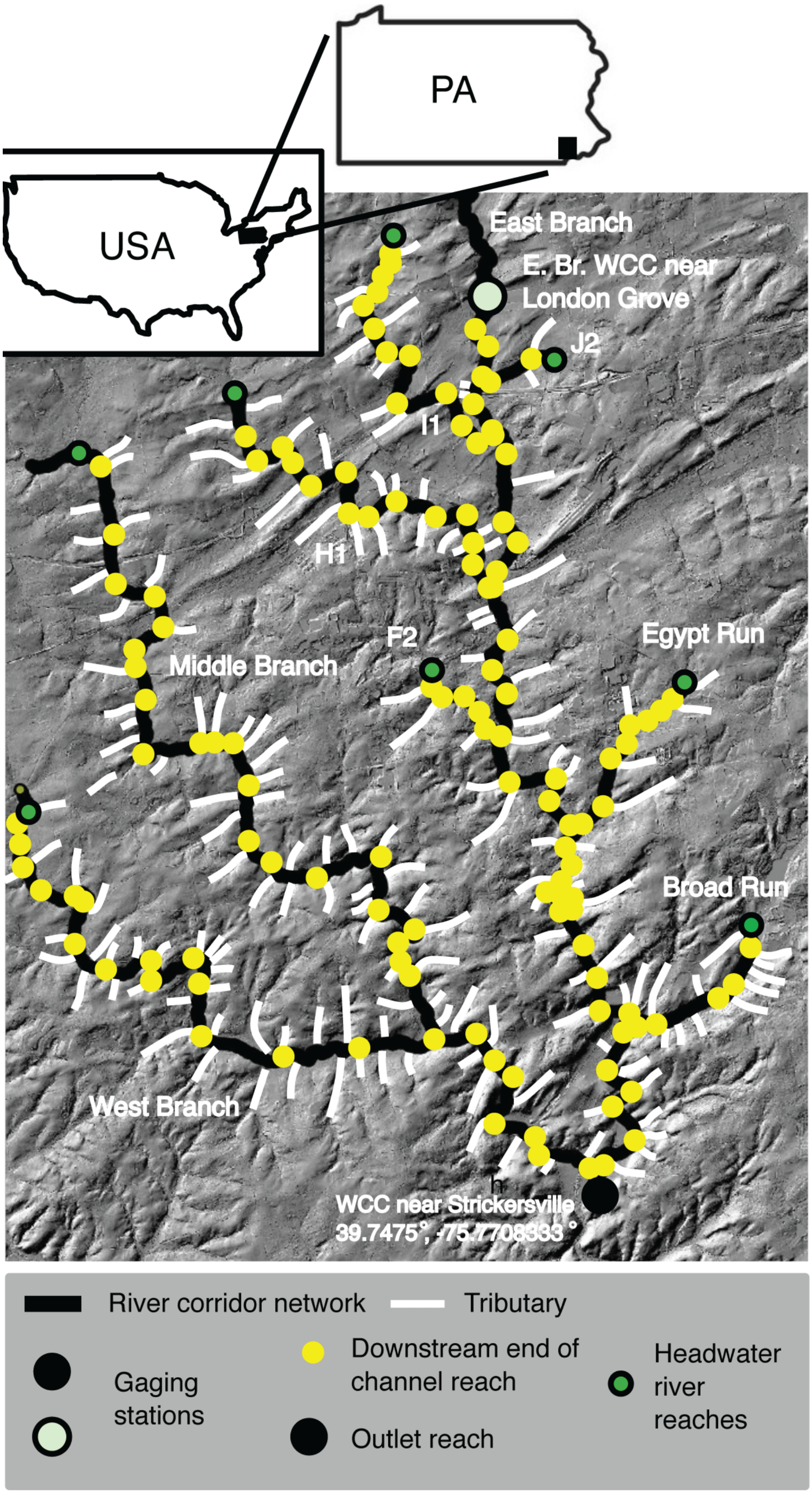

Figure 1 White Clay Creek watershed stream network with locations of channel sediment budget reaches and USGS stream gaging stations White Clay Creek near Strickersville and East Branch White Clay Creek near London Grove. Alphanumeric tributary names (F1, H2, etc.) were assigned for convenience during this study. Headwater reaches (defined in the text and illustrated by filled circles in two shades of green in Figure 1) are locations where the sediment budget only consists of tributary sediment inputs (e.g., bank erosion or floodplain deposition are not estimated for these reaches).

Gravel-sized sediment comprises most of the bed material, while much of the sediment load is composed of sand, silt, and clay transported in suspension (Bodek et al., 2021; McCarthy, 2018). River channels are typically bordered by active floodplains (Pizzuto et al., 2022, 2023). River deposits record anthropogenic influences on sedimentation, including legacy sediment deposits related to post-Colonial deforestation and poor agricultural practices (Costa, 1975; Jacobson and Coleman, 1986), and localized impacts of 18th- and 19th-century mill damming (Walter and Merritts, 2008; Pizzuto et al., 2023). Channel morphology obeys systematic hydraulic geometry relationships, indicating a quasi-equilibrium between channel form and the current hydrologic and sediment regime (Bodek et al., 2021; Wolman, 1955).

3 Methods

3.1 Sediment Budget Framework

Sediment budgets require defining spatial and temporal frameworks for analysis. The spatial framework consists of control volumes, which are then analyzed over a specific time interval. Here we use segments of the stream channel as control volumes, and define sediment budget components on an annual basis. Budgets are created for reaches of the mapped river corridor network of Fig. 1, which primarily includes the river channel and its adjacent floodplain. Headwater environments such as ravines, gullies, and tributary fans are not included (but these are discussed in Section 3.3).

To define locations and extents of stream channel control volumes, channel banks upstream of the USGS gaging station WCC near Strickersville were mapped by hand in an ARCGIS framework (Supplementary Materials, Table S1). At the beginning of the study in 2018, imagery from 2008 (Pennsylvania Spatial Data Access, 2025) was the best available that spanned the entire study area; these data were supplemented by a 1-meter resolution digital elevation model (U.S. Geological Survey, 2025a) and its associated hillshade. Banks were mapped upstream until channels became too small to resolve using the available imagery and DEM, resulting in the mapped channel network of Fig. 1. Any channel upstream of the mapped river network of Fig. 1 is defined as a headwater tributary channel for this study.

After the channel banks were mapped, 140 stream channel control volumes were defined by identifying sections of the river corridor with relatively uniform valley orientations. Control volumes vary in length from $\sim$100 to $\sim$1000 m; their downstream ends are illustrated in Fig. 1. Each control volume is associated with an adjacent floodplain where sediment is deposited during overbank flows. The control volumes and their adjacent floodplains together comprise 140 valley reaches of the channel network of the White Clay Creek (Supplementary Materials, Data Set S1).

Previous studies of the suspended sediment budgets of mid-Atlantic streams (Allmendinger et al., 2007; Donovan et al., 2015; Gellis et al., 2017; Hupp et al., 2013; Noe et al., 2020, 2022; Pizzuto et al., 2018; Schenk et al., 2013; Smith and Wilcock, 2015; Williamson, 2013) suggest that an annual sediment budget for the i^{th} channel control volume of the White Clay Creek can be written as

$$Q_{s\text{-}out_i} = BE_i - OD_i + HI_i + Q_{s\text{-}out_{i-1}} \quad (2)$$

where Q_{s-out_i} is the mass of sediment leaving channel control volume i per year (notation is summarized in the Supplemental Information, Text S7), BE_i is the mass of sediment supplied by bank erosion within control volume i per year, OD_i is the mass deposited on floodplains by overbank deposition, HI_i represents sediment input from headwater tributaries, and $Q_{s-out_{i-1}}$ represents sediment supplied from channel control volumes upstream of control volume i. Headwater tributaries include all channels that drain to the mapped network, whose banks could not be resolved visually and are therefore not included in mapping the channel network itself. For most control volumes, $Q_{s-out_{i-1}}$ is simply the output from the control volume immediately upstream, but where branches of the network join, $Q_{s-out_{i-1}}$ represents the contribution from two control volumes immediately upstream. Sediment supplied by reaches upstream of the 8 headwater reaches of Fig. 1 are treated as HI contributions, since these reaches have no mapped upstream reaches that could define values of $Q_{s-out_{i-1}}$. Equation 2 neglects suspended sediment stored within the channel, and sediment deposits associated with lateral migration are incorporated in the overbank deposition term. All variables in Equation 2 have units of Mg/yr.

Several different sources were used to identify the 166 headwater tributaries illustrated in Fig. 1. Every tributary to WCC contained in the NHD Plus High Resolution dataset (U.S. Geological Survey, 2025b) was included. Additional tributaries were identified from the ESRI World Topographic Map (ESRI, 2025). Tributaries not recognized from the other sources were also identified from the DEM; only channels clearly connected to the mapped channel of the White Clay Creek network were included.

If Eq. 2 is summed over all 140 channel control volumes, all the Q_{s-out} terms cancel except for the output from the downstream end of the watershed, $Q_{s-out_{140}}$. The resulting watershed-scale sediment budget is

$$Q_{s-out_{140}} = BE_t - OD_t + HI_t \quad (3)$$

where the subscript t indicates the sum of each variable over all channel control volumes; for example, $BE_t = \sum_{i=1}^{140} BE_i$. The sediment flux predicted by Eq. 3 is compared with the measured sediment flux at the Strickersville stream gaging station to evaluate the sediment budget methodology. Assessment of uncertainty and error propagation are discussed below.

3.2 Headwater Tributary Inputs

Williamson (2013) analyzed 19 years of data from the stream gaging station WCC Tributary above London Grove. She developed a sediment rating curve, and computed sediment fluxes for each discharge measurement using the rating curve. This analysis resulted in an annual suspended sediment flux estimate of 361 ± 77 Mg/yr. This value, scaled by drainage basin area, was used here as an estimate for all tributaries identified using the NHD HR Plus data and the World Topographic Map. The lengths of the tributaries identified from the World Topographic Map were measured and the drainage area determined using an empirical relationship between stream length and drainage basin area (see Supplementary Materials, Fig. S1 and Table S2). For tributaries identified from the DEM, nearly all of which represented very small watersheds, a constant sediment flux of 15 ± 3 Mg/yr was used. These methods for computing headwater tributary inputs are admittedly simplistic; errors that may arise are explored in the Discussion.

3.3 Hillslope–River Corridor Headwater Tributary Input Partitioning

The gaging station WCC Tributary above London Grove is located on a second-order stream channel. Sediment sampled at this location originates from upland areas such as hillslopes and gullies and locations within the river corridor, which could include sediment eroded from floodplains, banks, and sediment stored within the channel. To help watershed managers identify areas for siting Best Management Practices to reduce sediment loading, it is important to separate sediment supplied from upland slopes and gullies from sediment sourced from the river corridor. Karwan et al. (2018) and Rose et al. (2018a,b) sampled storm flows at the WCC Tributary above London Grove. Using geochemical fingerprinting and a mass balance analysis, they identified a threshold discharge required for upland sediment sources to provide sediment to the gaging station. Below this threshold, sediment is primarily sourced from within the river corridor. This threshold discharge is 0.97 (range: 0.78–1.28) m^3/s, a flow that has a recurrence interval of 0.93 months (29 days). These results imply that during events below the threshold discharge, sediment eroded from hillslopes and gullies is primarily stored in headwater landforms such as toeslopes, alluvial fans, and tributary floodplains. To partition the annual flux at the WCC Tributary above London Grove between upland and river corridor sources, Williamson's (2013) analysis was repeated using the threshold discharge as a purely binary discriminator. That is, for discharges below the threshold of 0.97 m^3/s, 100% of the sediment was assigned to river corridor sources (identified as "bank erosion" below), while for discharges above the threshold, 100% of the sediment was assigned to upland hillslope (HS) sources. Similar to the methods used to determine headwater tributaries supply, our approach for partitioning upland sediment supply between upland hillslopes and headwater river corridor sources is quite simplistic. Errors resulting from these methods are addressed in detail in the Discussion.

3.4 Measured Sediment Output Flux

Daily sediment discharge data for the WCC near Strickersville for water years 2011–2024 were downloaded from https://nwis.waterdata.usgs.gov. Data were summed for each year to determine the annual sediment flux (all yearly values are reported in the Supplementary Materials, Table S3). The mean annual suspended sediment flux for these years is 25 300 Mg/yr, with a standard deviation of 16 000 Mg/yr. The median, minimum, and maximum values are 28 300 Mg/yr, 3 400 Mg/yr, and 53 000 Mg/yr.

3.5 Bank Erosion

To determine values of bank erosion that can be used in the sediment budget (Eq. 2), a spatially comprehensive approach to estimating annual rates of bank erosion is required. This is accomplished 1) through a literature review of relevant studies in the region to guide an appropriate experimental design, 2) by assembling a database of measured bank erosion rates within the White Clay Creek and nearby watersheds, and 3) by creating an empirical model to predict bank erosion rates that relies on variables readily available throughout the WCC watershed.

3.5.1 A Conceptual Framework for Predicting Bank Erosion Rates

Previous studies of the region provide a useful basis for understanding bank erosion in the WCC watershed. The WCC's banks are frequently confined by bedrock and anthropogenic structures; where present, bedrock outcrops and engineering structures limit bank erosion rates (Bodek et al., 2021), as is typically observed along streams of the mid-Atlantic region (Pizzuto et al., 2018). Unconfined banks of the White Clay Creek are composed of cohesive clay, silt, and sand, with low organic content (Pizzuto et al., 2023). Channels are typically bordered by riparian forests or grasses and shrubs (McCarthy, 2018). Forested vegetation is associated with reduced bank erosion rates compared with grassy or herbaceous vegetation (Allmendinger et al., 2005; Hession et al., 2003; McCarthy, 2018; Pizzuto and Mecklenburg, 1989; Pizzuto et al., 2010). Freeze–thaw processes loosen soil particles and enhance bank retreat rates during the winter (Inamdar et al., 2018; Merritts et al., 2013; Pizzuto, 2009; Wolman, 1959; Wynn and Mostaghimi, 2006). Eroding banks are often located along the outsides of bends, suggesting a link between bank erosion and near-bank velocity or shear stress (Julian and Torres, 2006; McMillan and Hu, 2017; Pizzuto and Mecklenburg, 1989). High stream banks upstream of mill dams may locally enhance rates of bank erosion (Merritts et al., 2013), but Donovan et al. (2016) suggest that this is a relatively minor process in the Maryland Piedmont, a conclusion that may be extended to the WCC based on the paucity of millpond deposits preserved in the White Clay Creek's floodplains (Pizzuto et al., 2023). Median bank retreat rates are ∼5 cm/yr (Supplementary Materials, Table S4 presents bank erosion measurements of Allmendinger et al., 2005; Pizzuto and Mecklenburg, 1989; Rhoades et al., 2009; Schenk et al., 2013; Noe et al., 2020, 2022), so bank erosion should be measured on multidecadal timescales using precise methods.

3.5.2 Identifying Banks Confined by Bedrock and Anthropogenic Structures

Based on field observations, bank erosion rates were assumed to be negligible where banks were confined, necessitating a method for discriminating between confined and unconfined streambanks. This was accomplished by mapping confined streambanks at selected sites in the field (Supplementary Materials, Table S1), and developing an empirical topographic criterion to separate confined banks from unconfined banks.

ARCGIS tools provided the basis for developing a topographic criterion for identifying confined streambanks. First, discrete points were identified at 2-meter intervals along mapped streambanks, providing a total of 2 316 streambank points classified as either confined or unconfined based on field observations. Then, relief, R, was determined within a neighborhood of each bank point, with the size of the neighborhood scaled by bankfull channel depth, D_{bf} (see Supplementary Materials, Text S1, Figs. S2–S8, and Table S5 for details). The following criterion for confinement was found to correctly classify 82% of the 2 316 field observations:

$$\frac{R}{D_{bf}} > 1.7 \tag{4}$$

3.5.3 Empirical Approach For Computing Mass Erosion Rates of Unconfined Streambanks

Several steps led to an approach for estimating bank erosion rates of unconfined streambanks throughout the WCC watershed (Supplementary Materials, Table S1). ARCGIS routines were used to create channel centerlines at 2-meter intervals from the mapped banklines; curvature was computed for each centerline point using methods of Blanckaert and de Vriend (2010). Then, estimates of decadally averaged rates of bank retreat were compiled for the WCC and neighboring watersheds from McCarthy (2018), Allmendinger et al. (2005), and Pizzuto and Mecklenburg (1989); see Supplementary Materials, Table S4. To avoid bias associated with previous studies' focus on highly active eroding banks, 12 additional locations were included for the WCC where banks appeared to be stable (i.e., not eroding) based on criteria of Pfankuch (1975). For each location, additional explanatory variables were also compiled. Bankfull width was available from previous studies or (for new data from the WCC) estimated based on nearby measurements reported by McCarthy (2018). Curvature for White Clay Creek sites was computed as described above. Curvatures for sites of Allmendinger et al. (2005) and Pizzuto and Mecklenburg (1989) were estimated from maps included in the original publications. Canopy cover was estimated using the 30-meter resolution NLCD 2016 Tree Canopy L48_20190831 (CONUS) data set, described by Yang et al. (2018).

These data (summarized in Supplementary Materials, Table S4) lead to a non-linear equation to compute bank erosion rates, BE_L (with units of cm/yr):

$$BE_L = \frac{W_{BF}C}{(0.004137 + 0.006519F^{0.3})} \tag{5}$$

where W_{BF} is the bankfull width (in meters), C is the channel curvature (units of 1/m), and F is the canopy cover as a percentage. Eq. 5 has an adjusted r^2 of 0.57 and an RMSE of 7.312 cm/yr. The mean observed erosion rate is 9.1 cm/yr, so scaling the RMSE by the mean yields a fractional mean error estimate of 0.80, or 80%. The exponent 0.3 on F is imposed, rather than determined by the non-linear regression. Plotting observed and predicted erosion rates suggests that Eq. 5 tends to underestimate relatively higher erosion rates, i.e., those between 25 and 40 cm/yr (Supplementary Materials, Fig. S9), an observation which resists facile explanation beyond noting that our approach may neglect some important variables.

Eq. 5 was used to estimate bank erosion rates throughout the WCC mapped channel network. Bankfull width was estimated using a relationship between width and maximum channel length upstream (Supplementary Materials, Fig. S10). Linear bank erosion rates were converted to mass units by multiplying by the 2-meter point spacing, the local bank height (Supplementary Materials, Fig. S11), and the depth-averaged bulk density of 1.3 ± 0.09 g/cm^3 obtained from 72 WCC samples (see Supplementary Materials, Figs. S11 and S12, and Table S6). This approach assumes that the entire bank height consists of relatively fine-grained sand, silt, and clay that can be transported in suspension after erosion. The low standard deviation of bulk density supports the use of a constant depth-averaged value. Detailed bank descriptions and sediment analyses justify these assumptions (Bodek et al., 2021; McCarthy, 2018; Pizzuto et al., 2022, 2023).

3.6 Floodplain Sedimentation

Annual floodplain sedimentation was computed for each of the 140 valley reaches of the White Clay Creek watershed following the 15 steps outlined in Supplementary Materials, Table S7. The approach is summarized briefly here, with additional details presented in the Supplementary Materials (Text S5).

Linear floodplain sedimentation rates were compiled from published (Marquard, 2015; Pizzuto et al., 2022) and unpublished sources, yielding estimates for 10 locations in the WCC watershed (Supplementary Materials, Text S5.1 and Table S8). Sedimentation rates are uncorrelated with potential explanatory variables such as canopy cover (Pizzuto, 2012), drainage basin area, or valley slope, so an average value of 0.40 ± 0.33 cm/yr was used throughout the entire watershed. Because most measurements were obtained close to the channel of the White Clay Creek, and because natural levees are common throughout the WCC watershed, results of Pizzuto (1987) for the nearby Brandywine Creek were used to account for the decrease in floodplain sedimentation rate with increasing distance from the channel. This resulted in multiplying the constant value of 0.40 cm/yr by a factor of 0.7 at all valley reaches (Supplementary Materials, Text S5.2).

The area of floodplain inundation was determined following steps 5–14 of Table S7 (detailed in the Supplementary Materials, Text S5.3 and S5.4). A representative cross-section was extracted from the DEM, and the valley slope was estimated from the channel's bed slope, adjusted for channel sinuosity. The water surface elevation of the 10-year flood at the cross-section was computed using Pizzuto's (2012) 1-D hydrodynamic model, calibrated to the rating curve obtained at the USGS gaging station WCC near Strickersville. The fraction of the inundated area corresponding to the active floodplain was estimated from these results (Supplementary Materials, Fig. S15), and the plane of the sloping water surface within the valley reach was determined. A 0.3-meter square grid was superimposed throughout the valley reach in ARCGIS, and the elevations of each point extracted from the DEM. Comparison of the elevations of these points with the planar 10-year water surface determined the number of points inundated by the 10-year flood. Points within the channel and outside the active floodplain were removed to determine the area of overbank sedimentation within the valley reach.

The mass of sediment deposited on the floodplain in each valley reach per year was then obtained by multiplying the area inundated by the 10-year flood with the corrected linear sedimentation rate and the floodplain bulk density (from Section 3.4.3 above).

3.7 Fraction of Bank Erosion Comprised of Legacy Sediment

In the mid-Atlantic region, the term "legacy sediment" describes deposits in river corridors created as a result of anthropogenic activities following European settlement (James, 2018). Legacy sediments comprise a significant thickness of alluvium in mid-Atlantic river corridors, and erosion of these deposits is often considered a potential water quality issue (Donovan et al., 2015; Hupp et al., 2013; Jacobson and Coleman, 1986; Lutgen et al., 2020; Merritts et al., 2013; Noe et al., 2020).

To estimate the contribution of legacy sediment to the sediment budget of the White Clay Creek, a chronology for legacy sediment is needed. Pizzuto et al. (2022, 2023) defined legacy sediments as those deposited between 1750 and 1950. These two chronostratigraphic horizons have previously been determined for 6 locations in the WCC watershed (Supplementary Materials, Table S9). These data, along with bank-height measurements, resulted in 6 estimates of the fraction of eroding banks comprised of legacy sediments. The mean and standard deviation of legacy sediment fractions (presented in Results, below) were used to estimate the legacy sediment contribution from bank erosion to the sediment budget of the WCC.

3.8 Nesting Sediment Budgets to Route Sediment From Specific Sources Downstream

Sediment entering a channel reach of the WCC can follow two different paths. Some sediment can be stored on floodplains, while other sediment can be carried out of the reach and into the next reach downstream. Because each channel reach has its own empirically determined local sediment budget, the fraction of incoming sediment that follows each path can be determined. By continuing these computations from a specific location through nested reaches downstream, the fate of sediment from any source in the watershed can be determined. In particular, the contribution from any source to the watershed's outlet sediment flux can be quantified.

Three assumptions facilitate computations. First, all sediment entering a channel reach is considered as equally likely to be either deposited on a floodplain or transported downstream, i.e., sediment within the channel reach is treated as "well-mixed". Second, sediment eroded from banks within a channel reach is not redeposited within the same valley reach, but is carried into the immediately adjacent channel reach downstream. Third, sediment deposited on a floodplain is not remobilized within the 1-year time frame of the sediment budget.

The first step in computing the downstream fate of sediment from any source is to define a path from the source to the basin's outlet. A sequence of numbers, P_i, is used to identify the N_i channel reaches (each denoted by a unique number i_j) traversed in order from source channel reach i_0 to the basin outlet at channel reach 140:

$$P_i = i_0, i_1, i_2 \ldots i_j \ldots 140_{N_i} \tag{6}$$

The flux of any quantity of sediment leaving control volume i_0 and entering the first downstream reach i_1 is denoted X_{si_0}. The fraction of sediment stored within reach i_1, FS_{i_1}, is determined from its local sediment budget:

$$FS_{i_1} = \frac{OD_{i_1}}{Q_{s-out_{i_0}}} \tag{7}$$

The amount of X_{si_0} that is stored in reach i_1 is then

$$X_{si_0}^{\text{stored}} = (FS_{i_1})(X_{si_0}) \tag{8}$$

Similarly, the amount of X_{si_0} leaving reach i_1, which can be denoted X_{si_1}, is

$$X_{si_1} = (1 - FS_{i_1})(X_{si_0}) \tag{9}$$

Eq. 9 can then be applied recursively along the path P_i to determine how much of the flux X_{si_0} remains after being transported downstream along the path to reach i_j.

$$X_{si_j} = (X_{si_0}) \prod_{k=1}^{j} (1 - FS_{i_k}) \tag{10}$$

Note that all the terms under the product sign are < 1, indicating that as sediment is carried progressively downstream, the amount of sediment remaining will continue to decrease. This occurs because sediment is removed within each reach by overbank deposition, implying that sources in the headwaters of the drainage basin will contribute less sediment to the watershed's sediment yield than sources close to the basin outlet.

If both sides of Eq. 10 are divided by the initial sediment flux X_{si_0}, a dimensionless variable P_{rob} can be defined:

$$P_{\text{rob}} = \prod_{k=1}^{j} (1 - FS_{i_k}) \tag{11}$$

P_{rob} can be interpreted as the probability that a particle originating in channel reach i_0 will reach channel reach i_j within a year.

3.9 Quantifying Uncertainty

Uncertainty arises for estimates of individual sediment budget components within each channel reach. Additional errors arise from the quantities computed from individual budget components, including the sediment budget for the entire watershed obtained by summing individual reach-scale budget components and the downstream routing computations outlined in Section 3.8 above. Here methods for assessing error are outlined in brief; a more detailed account is presented in the Supplementary Materials, Text S6. Uncertainty in computing the watershed output flux is assessed by the standard deviation of the annual sediment flux measured at the gaging station WCC near Strickersville, PA. The mean and standard deviation of the annual fluxes at this gaging station are 25 300 and 16 000 Mg/yr, respectively, for a fractional uncertainty of 0.63. This assessment of uncertainty only reflects annual variability and does not account for measurement error, so it represents a minimum estimate of uncertainty in the outlet sediment flux. Uncertainty in the headwater input flux at gaging station East Branch WCC Tributary near Avondale is reported by Williamson (2013). To estimate uncertainty, rating curve errors were assessed for each individual discharge, and then errors were summed following standard rules of error propagation (LibreTexts, 2025). Williamson (2013) reports a mean annual flux of 361 Mg/yr with a standard deviation of 77 Mg/yr, values that indicate a fractional uncertainty of 0.21. This constant fractional uncertainty was used to assess uncertainty in all headwater input fluxes, appropriately scaled for varying drainage basin area. Uncertainty in quantifying annual floodplain deposition in valley reaches is assessed from the mean and standard deviation of measured vertical accretion rates in the WCC watershed, which are 0.40 and 0.33 cm/yr, values that yield a fractional uncertainty of 0.83. This approach neglects substantial uncertainty in assessing the area of floodplain sedimentation in each valley reach, which cannot be rigorously evaluated. As a result, the value of 0.83 should be considered a substantial underestimate of the true uncertainty in floodplain deposition. Estimating uncertainty in bank erosion rates is more complex. Bank erosion is assessed at 2-meter intervals along each bank in a channel reach. The first step in estimating erosion is to determine if the bank is confined or unconfined, a decision that is wrong 18% of the time. Then, if the bank is unconfined, linear bank erosion rates are assessed using Eq 5, and the result is multiplied by the bank height and bulk density. Estimates of linear erosion rate, bank height, and bulk density have a collective uncertainty of 85%. Errors for individual 2-meter bank segments are then summed throughout each channel reach, following rules of error propagation, to obtain error estimates for the annual bank erosion flux for each channel reach. The equations used to perform this analysis are presented and explained in the Supplementary Materials, Text S6.2. Other results presented below are derived from the individual reach-scale sediment budget variables (i.e., headwater sediment inputs, bank erosion, and overbank deposition) of Eq. 2. Uncertainty in results derived from the individual reach-scale variables are obtained by propagating errors associated with each reach-scale variable through the computations.

4 Results

4.1 Sediment Budget Data For Individual Channel Reaches

Maps showing individual sediment budget components and the net budget obtained by summing these components for all watershed channel reaches identify hot spots of sediment production and storage (Fig. 2). Headwater input values (Fig. 2a) are high at the upstream ends of the network, a few channel reaches of the West Branch (where Bodek et al. (2021) noted a migrating knickpoint that has created locally steep topography), and at a small number of channel reaches scattered throughout the watershed. Bank erosion appears to be more uniformly distributed, with a few local hotspots (Fig. 2b). Floodplain deposition is generally low in headwater reaches, with the higher values closer to the watershed outlet (Fig. 2c). Several reaches along the lower West Branch appear to be deposition hotspots, likely due to unusually wide and straight valleys (resulting from local geological controls) that create large areas for floodplain sedimentation. Reach sediment budgets average $\sim$100 Mg/yr (Fig. 2d and 2e). Some headwater reaches have a net budget of over 500 Mg/yr (possibly because storage is not considered upstream of the channel network), while the net budget for others is negative due to high rates of floodplain deposition. Fractional errors in reach budgets are highly variable, averaging around 0.2 but ranging from 0.1 to 32 (Fig. 3). A few large fractional errors arise because the net budget is close to zero for some locations, resulting in large error ratios when errors are divided by very small net budget values. The cumulative sediment flux at each valley reach (from Eq. 3 applied to each reach rather than the outlet of the basin) illustrates how sediment flux accumulates downstream (Fig. 4a and 4b). The sediment flux from the upper third of the network remains around 2 000 Mg/yr. Sediment flux in the East Branch White Clay Creek exceeds that of the other two branches, reaching values of around 6 000 Mg/yr about halfway downstream to the watershed outlet. Fractional errors in the cumulative sediment budget average around 0.2 in headwater reaches, decreasing to 0.05 near the watershed outlet (Fig. 4b).

4.2 Routing Sediment Flux Components Through the Watershed

When headwater sediment fluxes are routed downstream using Eq. 10, they decrease as some sediment is progressively stored on floodplains. Figure 5 demonstrates that the decrease can be substantial, suggesting that relatively little sediment supplied from the headwaters will reach the outlet of the watershed. This observation is quantified in Fig. 4c and 4d, which map the fraction of the sediment supplied in each channel reach

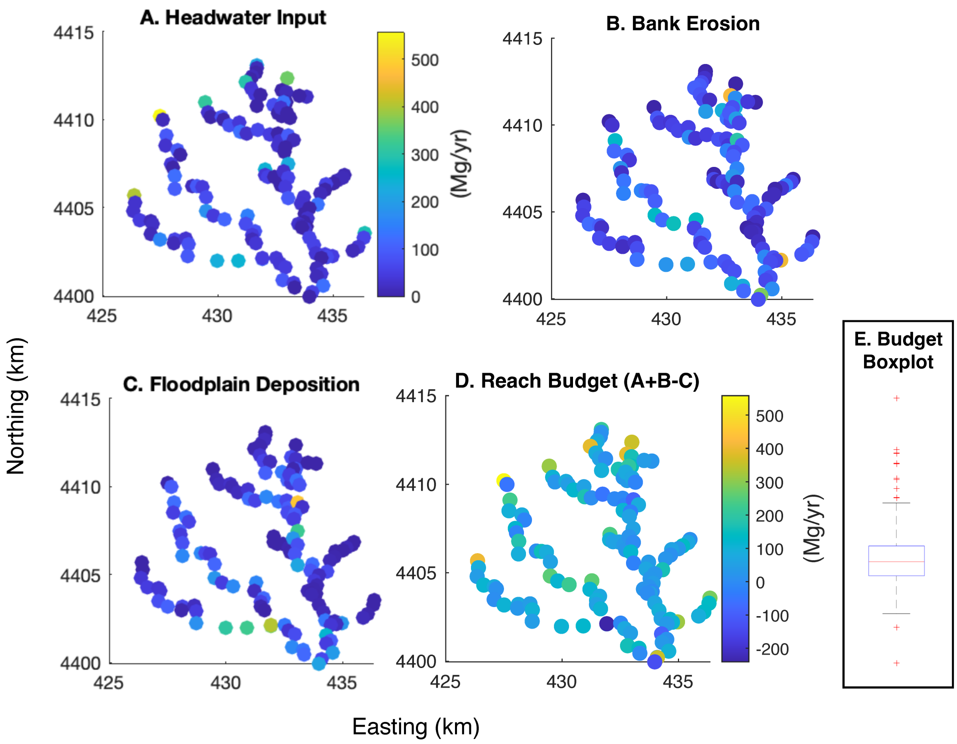

Figure 2 Sediment budget components for 140 channel reaches of the WCC. Symbols denote the downstream limit of each channel reach. **A**) Headwater input. Note that the colorbar for a also applies to panels b and c. **B**) Bank erosion. **C**) Floodplain deposition. **D**) Reach-scale sediment budget computed as headwater input + bank erosion − floodplain deposition. **E**) Boxplot of reach-scale budget values (aligned with the scale of the colorbar in d). The center of the box defines the median value, while the lower and upper sides of the box define the 25th and 75th percentiles. Short horizontal lines delimit the 5th and 95th percentiles, and "+" denotes outliers.

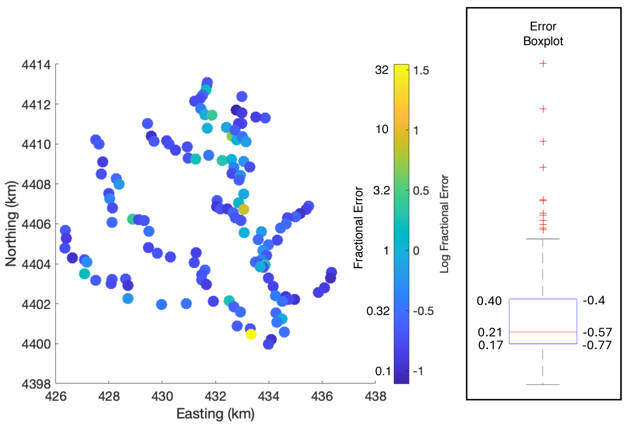

Figure 3 Map and boxplot of the logarithms (base 10) of the absolute values of the fractional errors of the net sediment fluxes (Fig. 2D,E) produced in each channel reach. For reference, the actual (non-logarithmic) fractional errors are provided for key values on the left sides of the colorbar and boxplot. Fractional errors are plotted as logarithms because some net fluxes are smaller than their absolute error terms, resulting in very large fractional errors.

that reaches the outlet of the basin (i.e., the variable P_{rob} defined by Eq. 11). Only about 20% of the sediment supplied in headwater channel reaches of the West, Middle, and East Branches of the White Clay Creek reach the outlet of the basin within a year. Values of P_{rob} progressively increase downstream, gradually approaching 1 near the watershed outlet. Fractional errors in these estimates are substantial (Fig. 4d), with some values near 1 in the headwaters and values of $\sim$0.2–0.6 elsewhere.

Routing the sediment supplied from each reach to the outlet of the basin also allows estimation of the fractional contribution from each reach to the watershed's sediment yield (Fig. 6). Most reaches within the White Clay Creek watershed contribute $\sim$1% towards the watershed's sediment yield, but a few hotspots contribute 2–3.5%. Hotspots of watershed sediment yield are mostly located in the lower reaches of the watershed.

4.3 Integrated Watershed-Scale Sediment Budget

The partitioning of the upland sediment flux at the U.S. Geological Survey's gaging station East Branch WCC Tributary above London Grove indicates that 76% of the headwater sediment input is supplied from upland sources, with 24% from bank erosion. When these results are combined with the individual sediment budgets for all reaches, and the results are summed, the watershed-integrated sediment budget of Table 1 and Fig. 7 is obtained. Bank erosion is the largest component (1.35 ± 0.05 times the computed watershed output), with floodplain deposition representing 0.89 ± 0.04 and headwater input representing 0.54 ± 0.02 times the computed output. The computed output of 11 710 (11 330–12 090) Mg/yr is within the uncertainty envelope of 9 300–43 000 Mg/yr of the measured output, so the predicted output is consistent with available measurements. However, the measured mean annual sediment flux of 25 300 Mg/yr is 2.2 times greater than sediment flux determined by solving the sediment budget equations.

When all sources are routed downstream to account for deposition on floodplains using Eq. 10, bank ero-

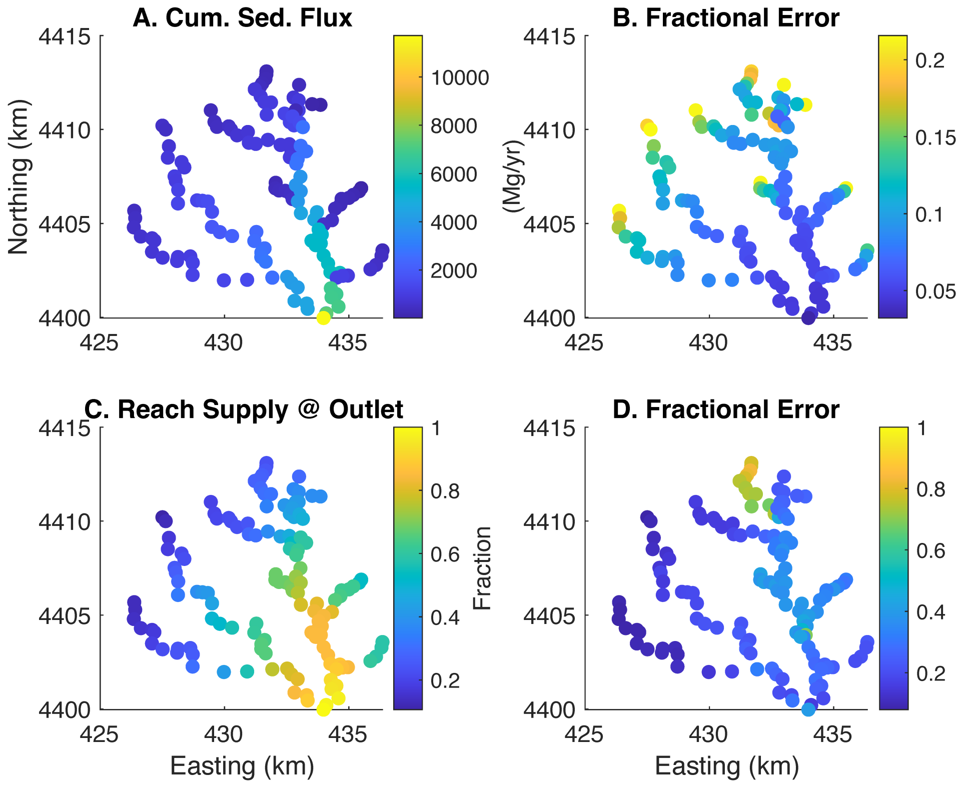

Figure 4 Upper two panels present the cumulative sediment flux leaving each channel node (panel A) and the associated fractional errors (panel B). Lower two panels present the fraction of the headwater input supplied to each node that remains at the outlet of the basin (panel C, "Reach Supply @ Outlet") and the associated fractional errors (panel D). The fractional reach supply at the watershed outlet (panel C) is the variable P_{rob} defined by Eq. 11.

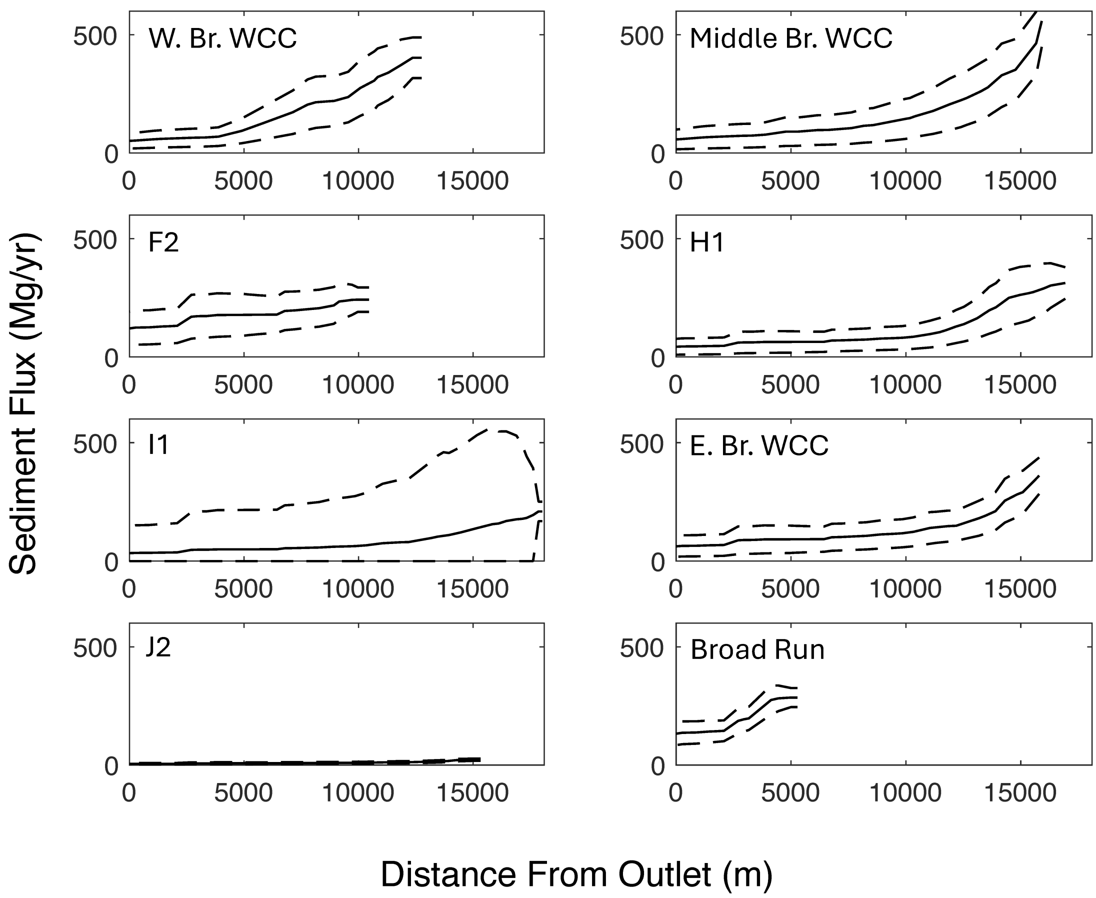

Figure 5 Sediment supply to 6 headwater reaches of the White Clay Creek (green circles in Fig. 1) and its progressive decrease through overbank deposition along the path to the outlet of the basin (filled black circle in Fig. 1). Solid lines indicate mean fluxes at each location, while the dashed lines represent ± 1 standard deviation around the mean. The value of each curve at a distance of 0 (i.e., at the basin outlet) represents the contribution of the headwater source to the sediment flux at the outlet of the White Clay Creek.

Table 1 Watershed-integrated sediment budget components computed from Eq. 3 and corresponding outlet contributions obtained by routing sediment downstream using Eq. 10 for the White Clay Creek (WCC) watershed. Measured Output represents the annual suspended sediment flux measured at the U.S. Geological Survey gaging station WCC near Strickersville. Headwater input is partitioned into Upland and Bank Erosion components using criteria developed by Rose et al. (2018a) and Rose et al. (2018b). Contributions from erosion of legacy sediments are also included. Particularly important results are highlighted in gray. Values in parentheses indicate uncertainty ranges.

Budget Component	Watershed Integrated Value (Mg/yr)	As Fraction of Computed Output	Component @ Outlet from Eq. 10 (Mg/yr)	Outlet Component as Fraction of Computed Output
Total Headwater Input	8290 (8060–8520)	NA	3770	NA
Headwater Input – Uplands	6300 (6130–6470)	0.54 (0.52–0.56)	2870	0.24 (0.22–0.27)
Headwater Input – Bank Erosion	1990 (1930–2045)	NA	900	NA
Non-Headwater Bank Erosion	13800 (13620–13980)	NA	7940	NA
Total Bank Erosion	15790 (15600–15980)	1.35 (1.30–1.40)	8840	0.76 (0.71–0.80)
Legacy Sediment Erosion	7100 (4900–9300)	0.61 (0.42–0.80)	3980	0.34 (0.28–0.40)
Floodplain Deposition	10380 (10140–10620)	0.89 (0.85–0.93)	NA	NA
Computed Output	11710 (11330–12090)	1.00 (0.95–1.05)	NA	NA
Measured Output	25300 (9300–41300)	2.20 (0.79–3.53)	NA	NA
Fraction of Headwater Input From Uplands = 0.76				
Fraction of Bank Erosion From Legacy Sediment = 0.45 (0.31–0.59)				

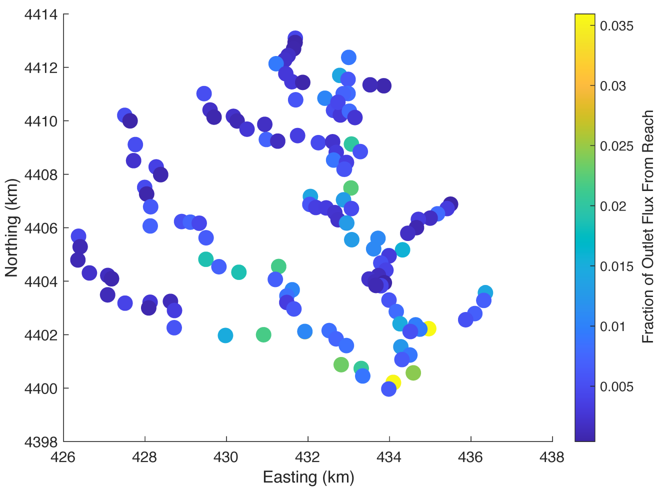

Figure 6 Fraction of the watershed sediment yield contributed by each channel reach.

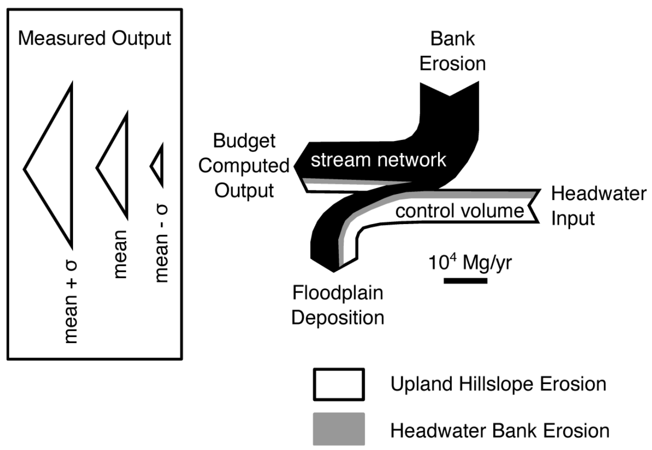

Figure 7 Graphical illustration of the watershed-integrated sediment budget, including contributions from upland hillslopes and headwater bank erosion. Boxed triangles (sized using the scale bar of the sediment budget) at left indicate statistics of the measured suspended sediment flux at the U.S. Geological Survey gaging station WCC near Strickersville, PA. The triangles provide a graphical comparison between the measured outlet flux and the outlet flux computed from the sediment budget.

sion accounts for $76 \pm 5\%$ of the watershed sediment flux, approximately three times the $24 \pm 3\%$ accounted for by upland headwater erosion. This implies that upland headwater inputs are preferentially stored on floodplains relative to bank erosion, likely because the headwater inputs (by definition) originate at the farthest distances from the basin outlet, enhancing the probability of sediment storage on floodplains as sediment moves downstream.

Table 1 also indicates that 45% (31–59%) of bank erosion in the WCC is comprised of legacy sediments. When bank erosion is routed downstream to the outlet of the basin, erosion of legacy sediments accounts for 34% (23–45%) of the watershed's annual sediment yield.

5 Discussion

Individual reach-scale sediment budget components are broadly similar in magnitude (~100–~300 Mg/yr; Fig. 2), with localized hotspots of sediment supply and storage. Because there are two input components (headwater tributary supply and bank erosion) and only a single sink (floodplain deposition), net budgets for individual reaches are nearly always positive (~100 Mg/yr), so cumulative annual fluxes increase downstream towards the outlet of the basin (Fig. 5a). Sediments supplied from individual channel reaches are progressively sequestered on floodplains as they move downstream, such that only ~20% of the sediment supplied from the far headwaters reaches the outlet of the basin (Figs. 4 and 5c).

After headwater tributary inputs are partitioned between upland hillslope sources and tributary bank erosion, bank erosion emerges as the largest component of the sediment budget, representing 1.35 times the measured output as compared to values of 0.54 and 0.89 for headwater input and overbank deposition, respectively (Table 1). Routing individual components downstream indicates that the bank erosion contribution to the outlet flux of 76% exceeds the 24% contributed by upland sources by a factor of $\sim$3. These results are consistent with results obtained elsewhere within the mid-Atlantic region (Noe et al., 2020). For example, Gellis et al. (2017) report a range of 23–82% for the bank erosion contribution to sediment yield for 8 mid-Atlantic watersheds, with an average value of 52%, somewhat lower than the 76% obtained here.

Stratigraphic data from 6 eroding streambanks of the WCC suggest that legacy sediment contributes 45 ± 14% to the total bank erosion component of the sediment budget of the WCC. Though based on limited data, this result is consistent with the value of 57 ± 16% for the legacy sediment contribution to bank erosion in Maryland reported by Donovan et al. (2015), and it is nearly identical to the average value of 47% obtained from Pizzuto's (2022) synthetic stratigraphic data for the mid-Atlantic Piedmont. Routing the contribution from legacy sediment downstream to the watershed outlet using Eq. 10 indicates that 34 ± 6% of the watershed sediment yield is comprised of legacy sediment.

5.1 Benefits and Limitations of the Nested Sediment Budget Approach

The nested sediment budget approach and its routing capabilities quantify the connectivity between all watershed locations and the basin outlet (Fig. 5c). This allows sediment sources to be connected to the outlet of the basin either by location or by category (e.g., bank erosion). For example, Table 1 quantifies contributions by both bank erosion and erosion of legacy sediment to the watershed sediment yield. Sediment contributions to the outlet flux have also been determined for all channel reaches in the WCC watershed (Fig. 6), potentially guiding watershed managers to select sites for restoration projects to reduce sediment loading.

However, all sediment budget computations presented above only represent snapshots of current conditions. In particular, the metric P_{rob} represents the contemporary behavior of the watershed only. It cannot represent future conditions, for example, those imposed by watershed restoration at a particular location, because restoration activities would change the parameters FS_{i_k} (fraction of the input load stored in a reach) in Eq. 10 and Eq.11 in unpredictable ways. Furthermore, sediment budgets represent annual sediment fluxes averaged over decades, and cannot therefore reflect temporal variability in the magnitude and frequency of storm events. Thus, while the nested sediment budget approach can prove useful in identifying locations to consider for watershed restoration, additional methods will be needed to predict the results of restoration designs implemented in specific locations in the watershed, particularly under changing hydrologic conditions caused by changes in land use or climate.

5.2 Evaluating Uncertainty

Sediment budgets are often plagued by substantial uncertainty, so errors are important to document and quantify (Grams and Schmidt, 2005; Grams et al., 2019; Kondolf and Matthews, 1991; Parsons, 2011), particularly when sediment budgets are designed to guide management decisions. For the WCC, sediment budgets of individual channel reaches have fractional errors that are typically $\sim$20%, but fractional errors can be much higher when the local sediment flux is low (Fig. 3). Routing sediment from individual sources downstream can create larger uncertainties (Figs. 4 and 5d), which appear to average $\sim$50% (Fig. 5d) but can be even higher. Fractional errors associated with the cumulative sediment flux are $\sim$20% in upstream reaches but decrease towards the outlet of the basin to $\sim$5% (Fig. 5b). Note that fractional errors decrease downstream because accumulating errors expressed as fractions vary by a factor of $N^{-1/2}$, where N is the number of measurements, and N increases downstream.

Despite a concerted effort to account for uncertainty and to propagate errors through all computations, important sources of error have been neglected. The sediment budget framework of Eq. 2, for example, may be incomplete, and neglected terms could influence sediment processes in the White Clay Creek watershed. The bank erosion model developed here assumes that no sediment is contributed through erosion of confined banks, but field observations suggest that this assumption is not always true. Further analysis of the distribution of confined banks, perhaps relying on surficial geological mapping, and studies of the erodibility of confined banks are needed. Computations of bank erosion estimate bank height based on a hydraulic geometry relationship because of limitations in interpreting local bank height from the DEM; this approach neglects systematic local variations in bank height that should be included in a more precise sediment budgeting approach. Important errors also arise from the methods used to determine the area of overbank sedimentation. The choice of the 10-year flood to represent flood discharges is arbitrary and perhaps difficult to justify as a general approach. The 1-D model for determining the elevation of the water surface during overbank flows, and its representation as a planar surface within a reach are both simplistic methods that could be improved. Our methods also treat headwater tributaries as uniform with regard to sediment production, a considerable idealization. All of these factors imply that the true uncertainties of the sediment budget are much larger than reported.

5.3 Avenues for Future Research

As suggested above, better methods are needed to estimate headwater sediment inputs. The approach followed here assumes that all upland watersheds, once scaled by drainage basin area, are identical to the watershed of the East Branch WCC Tributary near London Grove. However, local variations in geology, slope, soil type, land use, vegetation cover, and the occurrence of active gullies and other erosion hotspots likely influence input from headwater tributaries. Upland sediment storage and connectivity between sources and the channel network could also be included (Heckmann and Vericat, 2018). Furthermore, the method used to partition headwater sediment supply between upland hillslope and river corridor sources is also too simplistic. Our approach relies on a single threshold discharge, below which all sediment is supplied from bank erosion, and above which all sediment is supplied from hillslope erosion and other upland sources. This is clearly unrealistic, as both source categories should be active to some degree over all discharges. It would also be desirable to add more observations of bank erosion and floodplain deposition, and to decrease reliance on models of these processes. Models have been used to estimate bank erosion rates, and a simple basin-wide average has been used to represent floodplain deposition rates. However, it is not obvious how to increase the spatial coverage of direct measurements without greatly increasing the effort involved. The magnitudes of annual topographic change associated with erosion and deposition in the White Clay Creek watershed are small, on the order of decimeters or less for bank processes and millimeters for floodplain processes. For highly vegetated areas such as the White Clay Creek, these changes are too small to detect using repeat lidar measurements or structure-from-motion analyses of remotely sensed imagery, so labor-intensive point measurements of bank erosion and floodplain sedimentation are still required, as are methods to extrapolate these spatially. Developing improved methods to obtain these data should be a high priority for future research. Finally, automated workflows to map channel reaches and estimate their attributes would streamline creation of future nested sediment budgets. Previous studies suggest that the means of attaining this goal are already available (Baker et al., 2018; Jasiewicz and Stepinski, 2013; Lamont et al., 2019).

6 Conclusions

An annual suspended sediment budget for the 5th-order, 153.3 km^2 watershed of the WCC, Piedmont Province, southeastern Pennsylvania, U.S.A., quantifies relationships between headwater tributary input, bank erosion, floodplain sedimentation, and suspended sediment transport. Gaging station data provide estimates of sediment fluxes from headwater tributaries and at the outlet of the basin. To assess bank erosion, confined reaches were identified using a relief threshold, and erosion rates for the remaining unconfined reaches were determined using an empirical equation based on channel curvature and canopy cover. Floodplain sedimentation rates were averaged across the basin, and extrapolated across floodplains by modeling inundation by the 10-year flood. Previous sediment fingerprinting analyses suggest that 76% of headwater sediment fluxes are sourced from upland hillslopes, with the remaining 24% from headwater tributary streambanks. Stratigraphic observations (Pizzuto et al., 2022, 2023) suggest that $45 \pm 14\%$ of eroding banks consist of legacy sediments. After accounting for floodplain storage during downstream transport, eroded legacy sediments comprise $34 \pm 6\%$ of the total sediment flux from the watershed. The sediment budget is constructed by solving mass balance equations across 140 nested channel reaches. This approach identifies local variations in sediment production, storage, and transport, but more importantly, allows routing of sediment from any source downstream to the basin outlet, quantifying individual source contributions to the watershed sediment yield. Summing sediment budget components for each channel reach yields the traditional, basin-averaged sediment budget. Bank erosion is the largest component of the basin-averaged sediment budget (1.54 times the computed output), exceeding floodplain sedimentation (0.89 times the computed output) and hillslope erosion (0.54 times the computed output). The mean annual measured output at the U.S. Geological Survey's stream gaging station WCC near Strickersville (25 300 Mg/yr) exceeds the output computed from the sediment budget (11 710 Mg/yr) by a factor of 2.2, but the computed value is within the uncertainty range of the measurements (9 300–41 300 Mg/yr), so the sediment budget can be considered balanced. Routing sediments from all watershed sources downstream to the basin outlet provides additional insights. Because sediments are progressively stored on floodplains with increasing transport distance, only about 20% of the sediment supplied from the upper reaches of the watershed reaches the outlet of the basin within a year. Routing computations predict that bank erosion contributes 76% of sediment flux leaving the watershed, with upland hillslopes contributing the remaining 24%.

A common goal of sediment budgeting studies is to determine where sediments are sourced within a watershed. This information is needed to inform sediment management decisions to mitigate issues associated with excess sediment loading. Traditional spatially integrated sediment budgets, though they quantify the magnitudes of sediment budget components, fail to explicitly connect sediment sources to specific delivery locations. The nested sediment budget approach illustrated here provides a new, parsimonious method for providing this information.

Acknowledgements

Rejanne LeBivic and Nicholas Tobia helped assemble the geospatial database for the project. Dr. Stephanie Stotts assisted with dendrochronology. Comments from the Associate Editor, copyeditor Nari Miller, and two anonymous reviewers are appreciated and improved the manuscript considerably.

Land Recognition

The fieldwork was completed within areas of cultural significance to the Lenni Lenape indigenous people of the Northeastern Woodlands (https://en.wikipedia.org/wiki/Lenape).

Data and Codes Availability

MATLAB scripts and data files to create Figs. 2–6 are archived in Zenodo at https://doi.org/10.5281/zenodo.15813089. Two data files are included, one (`WCC_network_reach_budget_data.csv`) summarizing sediment budget and location data for each reach, and the other (`Adjacency_column_vector.csv`) indicating flow directions between reaches.

Funding Statement

Partial financial support was provided by Delaware Watershed Research Fund Award #DWRF-16-109.

Conflict of Interest Disclosure

The authors have no competing interests.

Permission to Reproduce Material from Copyrighted Sources

The authors declare that no material from copyrighted sources was reproduced in this manuscript.

Declaration on Artificial Intelligence Use

The authors declare that no artificial intelligence tool was used to assist in or generate any part of the contents in this manuscript.

References

Allmendinger, N. E., Pizzuto, J. E., Potter, N., Johnson, T. E., and Hession, W. C. The influence of riparian vegetation on stream width, eastern Pennsylvania, USA. *Geological Society of America Bulletin*, 117(1–2):229–243, 2005. doi: 10.1130/B25447.1.

Allmendinger, N. E., Pizzuto, J. E., Moglen, G. E., and Lewicki, M. A sediment budget for an urbanizing watershed, 1951–1996, Montgomery County, Maryland, USA. *Journal of the American Water Resources Association*, 43(6):1483–1498, 2007. doi: 10.1111/j.1752-1688.2007.00122.x.

Bainbridge, Z., Olley, J., Wilkinson, S., Bartley, R., Lewis, S., Dougall, C., Khan, S., Kuhnert, P., and Burton, J. Refining fine sediment source identification through integration of spatial modelling, concentration monitoring and source tracing: A case study in the Great Barrier Reef catchments. *Science of the Total Environment*, 892:164731, 2023. doi: 10.1016/j.scitotenv.2023.164731.

Baker, M., Saavedra, D., and Norton, M. Methodology for developing high-resolution stream and waterbody datasets for the Chesapeake Bay Watershed. Technical report, Chesapeake Bay Trust, 2018, https://cbtrust.org/wp-content/uploads/2018_Scope10_FinalReport_wAppendix.pdf.

Belmont, P., Willenbring, J. K., Schottler, S. P., Marquard, J., Kumarasamy, K., and Hemmis, J. M. Toward generalizable sediment fingerprinting with tracers that are conservative and nonconservative over sediment routing timescales. *Journal of Soils and Sediments*, 14:1479–1492, 2014. doi: 10.1007/s11368-014-0913-5.

Blanckaert, K. and de Vriend, H. J. Meander dynamics: A nonlinear model without curvature restrictions for flow in open-channel bends. *Journal of Geophysical Research*, 115:F04011, 2010. doi: 10.1029/2009JF001301.

Bodek, S., Pizzuto, J. E., McCarthy, K. E., and Affinito, R. A. Achieving equilibrium as a semi-alluvial channel: Anthropogenic, bedrock, and colluvial controls on the White Clay Creek, PA, USA. *Journal of Geophysical Research: Earth Surface*, 126(10): e2020JF005920, 2021. doi: 10.1029/2020JF005920.

Borah, D. K., Krug, E. C., and Yoder, D. C. Watershed sediment yield. In *Sedimentation Engineering: Processes, Measurements, Modeling, and Practice*, edited by Garcia, M. H., number 110 in ASCE Manuals and Reports on Engineering Practice, pages 827–858. American Society of Civil Engineers, Reston, VA, 2008. doi: 10.1061/9780784408148.

Church, M. and Slaymaker, O. Disequilibrium of Holocene sediment yield in glaciated British Columbia. *Nature*, 337:452–454, 1989. doi: 10.1038/337452a0.

Corrozi, M., Homsey, A., Kauffman, G., Farris, E., and Seymour, M. White Clay Creek State of the Watershed Report. Technical report, University of Delaware Institute for Public Administration, Water Resources Agency, Newark, DE, 2008.

Costa, J. E. Effects of agriculture on erosion and sedimentation in the Piedmont Province, Maryland. *Geological Society of America Bulletin*, 86(9):1281–1286, 1975. doi: 10.1130/0016-7606(1975)86<1281:EOAOEA>2.0.CO;2.

Donovan, M., Miller, A., Baker, M., and Gellis, A. C. Sediment contributions from floodplains and legacy sediments to Piedmont streams of Baltimore County, Maryland. *Geomorphology*, 235: 88–105, 2015. doi: 10.1016/j.geomorph.2015.01.025.

Donovan, M., Miller, A., and Baker, M. Reassessing the role of milldams in Piedmont floodplain development and remobilization. *Geomorphology*, 268:133–145, 2016. doi: 10.1016/j.geomorph.2016.06.007.

ESRI. World Topographic Map. https://www.arcgis.com/home/item.html?id=6e850093c837475e8c23d905ac43b7d0, 2025.

Fischer, J. M., Riva-Murray, K., Hickman, R. E., Chichester, D. C., Brightbill, R. A., Romanok, K., and Bilger, M. D. Water Quality in the Delaware River Basin, Pennsylvania, New Jersey, New York, and Delaware, 1999–2001. Circular 1227, U.S. Geological Survey, Reston, VA, 2004.

Frings, R. M. and Ten Brinke, W. B. M. Ten reasons to set up sediment budgets for river management. *International Journal of River Basin Management*, 16(1):35–40, 2018. doi: 10.1080/15715124.2017.1345916.

Gellis, A. C. and Walling, D. E. Sediment-source fingerprinting (tracing) and sediment budgets as tools in targeting river and watershed restoration programs. In *Stream Restoration in Dynamic Fluvial Systems: Scientific Approaches, Analyses, and Tools*, edited by Simon, A., Bennett, S. J., and Castro, J. M., volume 194 of *Geophysical Monograph Series*, pages 263–291. American Geophysical Union, 2011.

Gellis, A. C., Myers, M. K., Noe, G. B., Hupp, C. R., Schenk, E. R., and Myers, L. Storms, channel changes, and a sediment budget for an urban-suburban stream, Difficult Run, Virginia, USA. *Geomorphology*, 278:128–148, 2017. doi: 10.1016/j.geomorph.2016.10.031.

Grams, P. E. and Schmidt, J. C. Equilibrium or indeterminate? Where sediment budgets fail: Sediment mass balance and adjustment of channel form, Green River downstream from Flaming Gorge Dam, Utah and Colorado. *Geomorphology*, 71: 156–181, 2005. doi: 10.1016/j.geomorph.2004.10.012.

Grams, P. E., Buscombe, D., Topping, D. J., Kaplinski, M., and Hazel, J. E. J. How many measurements are required to construct an accurate sand budget in a large river? Insights from analyses of signal and noise. *Earth Surface Processes and Landforms*, 44:

160–178, 2019. doi: 10.1002/esp.4489.

Hack, J. T. Physiographic Divisions and Differential Uplift in the Piedmont and Blue Ridge. Professional Paper 1265, U.S. Geological Survey, 1982.

Heckmann, T. and Vericat, D. Computing spatially distributed sediment delivery ratios: Inferring functional sediment connectivity from repeat high-resolution digital elevation models. *Earth Surface Processes and Landforms*, 43(7):1547–1554, 2018. doi: 10.1002/esp.4334.

Hession, W. C., Pizzuto, J. E., Johnson, T. E., and Horwitz, R. J. Influence of bank vegetation on channel morphology in rural and urban watersheds. *Geology*, 31(2):147–150, 2003.

Hupp, C. R., Noe, G. B., Schenk, E. R., and Benthem, A. J. Recent and historic sediment dynamics along Difficult Run, a suburban Virginia Piedmont stream. *Geomorphology*, 180–181:156–169, 2013. doi: 10.1016/j.geomorph.2012.10.007.

Inamdar, S., Johnson, E., Rowland, R., Warner, D., Walter, R., and Merritts, D. Freeze–thaw processes and intense rainfall: The one-two punch for high sediment and nutrient loads from mid-Atlantic watersheds. *Biogeochemistry*, 141(3):333–349, 2018. doi: 10.1007/s10533-017-0417-7.

Interagency Wild and Scenic Rivers Council. White Clay Creek, 2025, Accessed 1 July 2025, https://www.rivers.gov/river/white-clay.

Jacobson, R. B. and Coleman, D. J. Stratigraphy and recent evolution of Maryland Piedmont flood plains. *American Journal of Science*, 286:617–637, 1986. doi: 10.2475/ajs.286.8.617.

James, L. A. Ten conceptual models of large-scale legacy sedimentation: A review. *Geomorphology*, 317:199–217, 2018. doi: 10.1016/j.geomorph.2018.05.021.

James, L. A., Monohan, C., and Ertis, B. Long-term hydraulic mining sediment budgets: Connectivity as a management tool. *Science of the Total Environment*, 651(2):2024–2035, 2019. doi: 10.1016/j.scitotenv.2018.09.358.

Jasiewicz, J. and Stepinski, T. F. Geomorphons — A pattern recognition approach to classification and mapping of landforms. *Geomorphology*, 182:147–156, 2013. doi: 10.1016/j.geomorph.2012.11.005.

Julian, J. P. and Torres, R. Hydraulic erosion of cohesive riverbanks. *Geomorphology*, 76:193–206, 2006. doi: 10.1016/j.geomorph.2005.11.003.

Karwan, D. L., Pizzuto, J. E., Aalto, R., Marquard, J., Harpold, A., Skalak, K., Benthem, A., Levia, D. F., Siegert, C. M., and Aufdenkampe, A. K. Direct channel precipitation and storm characteristics influence short-term fallout radionuclide assessment of sediment source. *Water Resources Research*, 54:4579–4595, 2018. doi: 10.1029/2017WR021684.

Knox, J. C. Floodplain sedimentation in the Upper Mississippi Valley: Natural versus human accelerated. *Geomorphology*, 79: 286–310, 2006. doi: 10.1016/j.geomorph.2006.06.031.

Kondolf, G. M. and Matthews, W. V. G. Unmeasured residuals in sediment budgets: A cautionary note. *Water Resources Research*, 27 (9):2483–2486, 1991. doi: 10.1029/91WR01625.

Kottek, M., Grieser, J., Beck, C., Rudolf, B., and Rubel, F. World map of the Köppen-Geiger climate classification updated. *Meteorologische Zeitschrift*, 15(3):259–263, 2006. doi: 10.1127/0941-2948/2006/0130.

Lamont, S., Ahmed, L., Metes, M. J., Claggett, P. R., Hopkins, K. G., and Noe, G. B. Floodplain and Channel Evaluation Tool (FACET), Version 0.1.0, 2019.

Langland, M. and Cronin, T. M. A Summary Report of Sediment Processes in Chesapeake Bay and Watershed. Water-Resources Investigations Report 03-4123, U.S. Geological Survey, New Cumberland, Pennsylvania, 2003.

LibreTexts. Chemistry — Propagation of Error, 2025, https://chem.libretexts.org/Bookshelves/Analytical_Chemistry/Supplemental_Modules_(Analytical_Chemistry)/Quantifying_Nature/Significant_Digits/Propagation_of_Error.

Lutgen, A., Jiang, G., Sienkiewicz, N., Mattern, K., Kan, J., and Inamdar, S. Nutrients and heavy metals in legacy sediments: Comparisons with upland soils, and implications for water quality. *Journal of the American Water Resources Association*, 56(4): 669–691, 2020. doi: 10.1111/1752-1688.12842.

Marquard, J. *Assessing the anthropogenic impact on soil redistribution processes using radionuclides (10Be, 210Pb, 137Cs, and 7Be): A case study from the Christina River Basin, USA*. PhD thesis, University of Exeter, Exeter, United Kingdom, 2015.

McCarthy, K. E. Riverbank Erosion Rates in the White Clay Creek Watershed, Pennsylvania, 2018.

McMillan, M. and Hu, Z. A watershed scale spatially-distributed model for streambank erosion rate driven by channel curvature. *Geomorphology*, 294:146–161, 2017. doi: 10.1016/j.geomorph.2017.03.017.

Meals, D. W., Dressing, S. A., and Davenport, T. E. Lag time in water quality response to best management practices: A review. *Journal of Environmental Quality*, 39:85–96, 2010. doi: 10.2134/jeq2009.0108.

Merritts, D., Walter, R., Rahnis, M., Cox, S., Hartranft, J., Scheid, C., et al. The rise and fall of mid-Atlantic streams: Millpond sedimentation, milldam breaching, channel incision, and stream bank erosion. In *The Challenges of Dam Removal and River Restoration*, edited by De Graff, J. V. and Evans, J. E., volume 21 of *Reviews in Engineering Geology*, pages 183–203. Geological Society of America, 2013. doi: 10.1130/2013.4121(14).

Noe, G. B., Cashman, M. J., Skalak, K., Gellis, A., Hopkins, K. G., Moyer, D., Webber, J., Benthem, A., Maloney, K., Brakebill, J., Sekellick, A., Langland, M., Zhang, Q., Shenk, G., Keisman, J., and Hupp, C. Sediment dynamics and implications for management: State of the science from long-term research in the Chesapeake Bay watershed, U.S.A. *WIREs Water*, 7:e1454, 2020. doi: 10.1002/wat2.1454.

Noe, G. B., Hopkins, K. G., Claggett, P. R., Schenk, E. R., Metes, M. J., Ahmed, L., Doody, T. R., and Hupp, C. R. Streambank and floodplain geomorphic change and contribution to watershed material budgets. *Environmental Research Letters*, 17:064015, 2022. doi: 10.1088/1748-9326/ac6e47.

Parsons, A. J. How useful are catchment sediment budgets? *Progress in Physical Geography*, 36(1):60–71, 2011. doi: 10.1177/0309133311424591.

Pennsylvania Department of Conservation and Natural Resources. PaGEODE – Pennsylvania GEOlogic Data Exploration, 2025, Accessed 3 October 2025, https://www.gis.dcnr.state.pa.us/pageode/.

Pennsylvania Spatial Data Access. PAMAP Program – County Mosaics 2003–2006, 2025, https://www.pasda.psu.edu/uci/DataSummary.aspx?dataset=1125.

Pfankuch, D. J. Stream Reach Inventory and Channel Stability Evaluation: A Watershed Management Procedure. Technical report, USDA Forest Service, 1975.

Pizzuto, J. An empirical model of event scale cohesive bank profile evolution. *Earth Surface Processes and Landforms*, 34: 1234–1244, 2009.

Pizzuto, J., O'Neal, M., and Stotts, S. On the retreat of forested, cohesive riverbanks. *Geomorphology*, 116:341–352, 2010. doi: 10.1016/j.geomorph.2009.11.008.

Pizzuto, J., O'Neal, M. A., Narinesingh, P., Skalak, K., Jurk, D., Collins, S., and Calder, J. Contemporary fluvial geomorphology and suspended sediment budget of the partly-confined, mixed bedrock-alluvial South River, Virginia, U.S.A. *Geological Society of America Bulletin*, 2018. doi: 10.1130/B31759.1.

Pizzuto, J. E. Sediment diffusion during overbank flows. *Sedimentology*, 34:301–317, 1987. doi: 10.1111/j.1365-3091.1987.tb00779.x.

Pizzuto, J. E. Predicting the accumulation of mercury-contaminated sediment on riverbanks: An analytical approach. *Water Resources Research*, 48:W07518, 2012. doi: 10.1029/2012WR011906.

Pizzuto, J. E. and Huffman, M. E. Compact models assess the impacts of floodplain storage on suspended sediment delivery and restoration lag times: A Chesapeake Bay case study. *Water Resources Research*, 61:e2024WR039273, 2025. doi: 10.1029/2024WR039273.

Pizzuto, J. E. and Mecklenburg, T. S. Evaluation of a linear bank erosion equation. *Water Resources Research*, 25:1005–1013, 1989. doi: 10.1029/WR025i005p01005.

Pizzuto, J. E., Skalak, K., Benthem, A., Mahan, S. M., Sturchio, N., and Pearson, A. Spatially averaged stratigraphic data to inform watershed sediment routing: An example from the Mid-Atlantic United States. *Geological Society of America Bulletin*, 2022. doi: 10.1130/B36282.1.

Pizzuto, J. E., Huffman, M. E., and Symes, E. Pre- and postsettlement depositional processes and environments of the 3rd- to 5th-order White Clay Creek watershed, Piedmont Province, Pennsylvania and Delaware, USA. *Geological Society of America Bulletin*, 2023. doi: 10.1130/B37032.1.

Ramsey, K. W. The Geology of the Old College Formation along the Fall Zone of Delaware. Report of Investigations 69, Delaware Geological Survey, Newark, Delaware, 2005.

Reid, L. M. and Dunne, T. Sediment budgets as an organizing framework in fluvial geomorphology. In *Tools in Geomorphology*, edited by Kondolf, G. M. and Piégay, H., pages 357–382. John Wiley & Sons, Hoboken, New Jersey, 2016.

Renner, G. T. The physiographic interpretation of the fall line. *Geographical Review*, 17(2):278–286, 1927. doi: 10.2307/208229.

Rhoades, E. L., O'Neal, M. A., and Pizzuto, J. E. Quantifying bank erosion on the South River from 1937 to 2005, and its importance in assessing Hg contamination. *Applied Geography*, 29: 125–134, 2009. doi: 10.1016/j.apgeog.2008.08.005.

Rose, L. A., Karwan, D. L., and Aufdenkampe, A. K. Sediment fingerprinting suggests differential suspended particulate matter formation and transport processes across hydrologic regimes. *Journal of Geophysical Research: Biogeosciences*, 123: 1213–1229, 2018a. doi: 10.1002/2017JG004210.

Rose, L. A., Karwan, D. L., and Goodsey, S. E. Concentration–discharge relationships describe solute and sediment mobilization, reaction, and transport at event and longer timescales. *Hydrological Processes*, 32:2829–2844, 2018b. doi: 10.1002/hyp.13235.

Schenk, E. R., Hupp, C. R., Gellis, A. C., and Noe, G. B. Developing a new stream metric for comparing stream function using a bank–floodplain sediment budget: A case study of three Piedmont streams. *Earth Surface Processes and Landforms*, 38:771–784, 2013. doi: 10.1002/esp.3314.

Shenk, G. W. and Linker, L. C. Development and application of the 2010 Chesapeake Bay Watershed Total Maximum Daily Load Model. *Journal of the American Water Resources Association*, 49: 1042–1056, 2013.

Smith, S. M. C. and Wilcock, P. R. Upland sediment supply and its relation to watershed sediment delivery in the contemporary mid-Atlantic Piedmont (U.S.A.). *Geomorphology*, 232:33–46, 2015. doi: 10.1016/j.geomorph.2014.12.036.

Trimble, S. W. Changes in sediment storage in the Coon Creek Basin, Driftless Area, Wisconsin, 1853–1975. *Science*, 214: 181–183, 1981. doi: 10.1126/science.214.4517.181.

Turley, M., Hassan, M. A., and Slaymaker, O. Quantifying sediment connectivity: Moving toward a holistic assessment through a mixed methods approach. *Earth Surface Processes and Landforms*, 46(12):2501–2519, 2021. doi: 10.1002/esp.5191.

Turley, M., Hassan, M. A., Zimmermann, A., and Lian, O. Sediment source partitioning and budgeting over historical timescales in a glacierized, mountain catchment. *Journal of Geophysical Research: Earth Surface*, 129:e2024JF007819, 2024. doi: 10.1029/2024JF007819.

Turowski, J. M., Hovius, N., Wilson, A., and Horng, M.-J. Hydraulic geometry, river sediment and the definition of bedrock channels. *Geomorphology*, 99:26–38, 2008. doi: 10.1016/j.geomorph.2007.10.001.

University of Delaware Water Resources Center. White Clay Creek State of the Watershed, 2024, https://whiteclay.org/state-of-the-watershed.

U.S. Geological Survey. 3D Elevation Program, 2025a, https://www.usgs.gov/3d-elevation-program.

U.S. Geological Survey. NHDPlus High Resolution, 2025b, https://www.usgs.gov/national-hydrography/nhdplus-high-resolution.

Walter, R. C. and Merritts, D. J. Natural streams and the legacy of water-powered mills. *Science*, 319:299–304, 2008. doi: 10.1126/science.1151716.

Williamson, E. K. Effect of Particle Exchange on Suspended Sediment Transport Distances in the White Clay Creek, Pennsylvania. Master's thesis, University of Delaware, Newark, Delaware, 2013.

Wolman, M. G. The Natural Channel of Brandywine Creek. Professional Paper 271, U.S. Geological Survey, 1955.

Wolman, M. G. Factors influencing erosion of a cohesive river bank. *American Journal of Science*, 257(3):204–216, 1959.

Wynn, T. and Mostaghimi, S. The effects of vegetation and soil type on streambank erosion, southwestern Virginia, USA. *Journal of the American Water Resources Association*, 42:69–82, 2006.

Yang, L., Jin, S., Danielson, P., Homer, C., Gass, L., Bender, S. M., Case, A., Costello, C., Dewitz, J., Fry, J., Funk, M., Granneman, B., Liknes, G. C., Rigge, M., and Xian, G. A new generation of the United States National Land Cover Database: Requirements, research priorities, design, and implementation strategies. *ISPRS Journal of Photogrammetry and Remote Sensing*, 146:108–123, 2018. doi: 10.1016/j.isprsjprs.2018.09.006.